Procedia CIRP 90 (2020) 510–515

Contents lists available at ScienceDirect

Procedia CIRP

journal homepage: www.elsevier.com/locate/procir

27th CIRP Life Cycle Engineering (LCE) Conference

Energy, time and material consumption modelling for fused deposition modelling process

Jimeng Yang, Ying Liu*

School of Engineering, University of Glasgow, Glasgow, G12 8QQ, United Kingdom

ARTICLE INFO

Keywords:
Additive manufacturing
Fused deposition modelling
G-code
Energy consumption
Time consumption
Material consumption

ABSTRACT

Additive manufacturing (AM) provides an evolutionary paradigm for the next generation of manufacturing. However, the understanding of AM's pattern is not sufficient in manufacturing time, energy and material consumptions. This study aims to provide a flexible and modular modelling method for the aforementioned indicators based on the path planning code and machine characteristics. It enables an accurate consumption prediction from an arbitrary manufacturing task at prefabrication phase and allows users to customise parameters to reduce consumptions. With a small number of experiments on different machine, this method is suitable for other related manufacturing technologies using numerical control programming.

1. Introduction

Additive Manufacturing, also known as 3D Printing (3DP), is defined as the material deposition process of a three-dimensional (3D) model based on the layer-slicing principle (Yang et al., 2017; Huang et al., 2016). Compared with conventional manufacturing (CM), this unique fabricating approach largely simplifies and accelerates the production process without the requirements of molds, dies and tools (Kellens et al., 2017). Its feature of rapid prototyping provides users with an efficient manufacturing environment with higher material utilisation and lower time consumption. As opposed to subtractive manufacture (SM) such as CNC machining, AM is conducive to both thin-skin and light-weighted production with an alternative infill density and a higher material usage efficiency, rather than solid fabrication (Chua C and Leong K, 2014; Ford and Despeisse, 2016). The design freedom with limitless geometric constraints offers AM a broad application into customised productions, which allows users to personalise the processing parameters. To produce complex designs, AM avoids the tooling-related constraints with the assist of support structure, especially for the consolidation of assemble parts. Since AM implements fabrication in terms of pre-defined path-planning code, it drives the production mode into mass customisation of high-differentiated products on-demand, which guarantees the high efficiency in future Industry 4.0 (Huang et al., 2016).

Due to the outstanding competitiveness, AM has profound impacts on numerous domains such as medicine, architecture, mechanics, aeronautics, chemical industry, education, food and social culture. It has been expanded into a wide variety of branches based on material feed and material process systems, ranging from powder bed fusion to material extrusion, from material deposition to sheet lamination, from thermal melting to light polymerisation (Kellens et al., 2017). Many manufacturers have dedicated to developing AM mechanism and its supporting software to provide consumers an easy-to-use, high-dominated, and customised operation environment. However, this emerging production mode still has weaknesses in manufacturing speed, energy and material consumptions.

2. Literature review

Whether AM is veritable as called "rapid prototype" is still doubtable. For mass customised production, AM mechanism is a limited factor itself as it consumes certain times on nozzle travelling, component heating and cooling down as well as its "job by job" mode. Against this issue, a relaxation scheme proposed by (Fok K et al., 2016) developed a path optimiser to shorten the extruder traversing time of each layer. Simulation results proved that the optimiser could significantly reduce the average time consumption in prefabricating and printing processes by nearly 10%. Another study in (Li et al., 2017) proposed a production planning

* Corresponding author.
E-mail addresses: j.yang.4@research.gla.ac.uk (J. Yang), Ying.Liu@glasgow.ac.uk (Y. Liu).

https://doi.org/10.1016/j.procir.2020.02.130

model to estimate production time and cost of specific AM machines by considering multiple factors, including design geometry, task and machine allocation, machine characteristics.

Energy sustainability has become an important topic in recent decades. A related study outlined available research on the environmental performance of AM, including the analyses of energy and resource consumptions. Detailed statistics on various AM processes compared with CM were performed. The results confirmed that AM system had a higher electrical energy demand, in which the energy required for direct metal deposition, direct laser deposition, FDM and selective laser melting (SLM) was higher than the average level (Kellens et al., 2017). Post-treatment on AM parts also need to be considered. For instance, a study in (Balogun et al., 2015) measured both time and energy consumed by ultrasonic cleaning to clean and remove the support material of FDM built part. The average power value was approximately 250 W. Another study in (Yoon H et al., 2014) compared energy consumptions of conventional bulk-forming, SM, and selective laser sintering (SLS). Statistical results illustrated that SLS consumed much higher in actual production if considering the entire AM process chain (Chua C and Leong K, 2014; Ford and Despeisse, 2016; Peng and Sun, 2017). The calculation of energy consumption requires precise estimation methods. A related study in (Meteyer et al., 2014) proposed a Unit-Process level model to estimate the energy consumptions of Binder-Jetting by measuring powers and times from basic-in-range energy-consuming parts, including print head, infra-red heater, curing oven, sintering process and idle state.

From the perspective of material consumption, a research by (Watson J and Taminger K M, 2015) proposed a decision-support model for comparing energy and material consumptions between AM and SM. A volume faction was obtained as a critical value to judge AM's feasibility. The result confirmed the weakness of AM, for instance, the poorly recycled material from the products with higher usage ratio of support.

Existing slicer software provides users with customised process parameters, such as layer thickness, support structure, product infill pattern, infill density, etc. Users may optimise both design and parameters to reduce consumed indicators. However, how to accurately model consumptions based on 3D design, machine characteristics and processing parameters; how to determine the most appropriate parameters to achieve the optimal consumptions require to be solved. Therefore, this study proposed a flexible and modular modelling method to predict time, energy and material consumptions of AM task at prefabrication stage. It aims to benefit the improvement of design part and assist users in customised selection of process parameters. To achieve a high-precision prediction, the initial model can be upgraded in terms of machine characteristics. The prediction method is expected to be applied in practical AM environment which is suitable for other related manufacturing techniques using numerical control (NC) programming.

3. Methodology

3.1. Framework for AM consumption prediction

Fig. 1 illustrates how a CAD design is improved throughout the loop of design and AM. A 3D design converted into computer aided manufacturing (CAM) is manufactured in terms of pre-defined process parameters. This is how a G-code file is generated. G-code, also called preparatory codes, is known as a generic programming language that is widely applied in computer numerical control (CNC). It works as input instructions to realise the automated control of machine tools for example milling machines, drills, electric discharge machining (EDM), lathes, AM printers, etc. (Apro, 2008). In the case of 3DP, the toolpath on each layer is formulated and written as G-code format according to the design geometry and

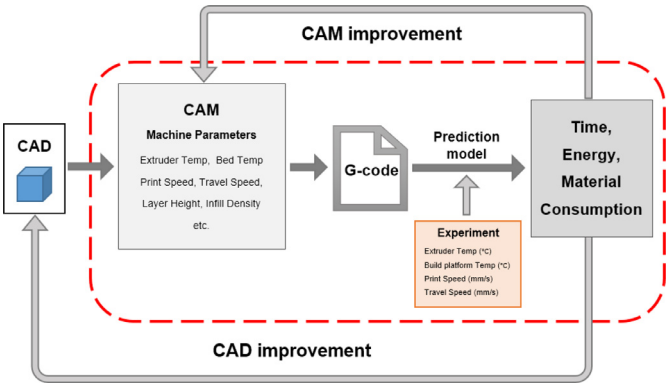

Fig. 1. Schematic of AM consumption prediction and design improvement.

slicing parameters. Table 1 presents all types of G-code commands generated from Cura, a general and open-source slicer software that supports general FDM printers on market. Printers may execute each command line by line to finish the print tasks.

In the industrial environment, it is unable to predict accurate consumptions only through a CAD design in prefabrication stage. Since importing the same design into different AM machines may produce print objects with different consumptions. All information relies on the machine specifications and working properties. Therefore, this study proves a specific method with a highly flexible and scalable predictive model that can calculate time, energy and material consumptions based on the generated G-code. The method is feasible for any other manufacturing machines working by G-code and is expected to be applied into related CNC manufacturing techniques. However, it is impossible to build up a unified model due to the machine difference. Hence a brief framework of building the prediction model is proposed at first. In practical case studies, the models can be upgraded and refined based on the major working components from tested AM machines with the assist of experiments.

Modelling starts with FDM process, which is an affordable and commonly applied branch of AM technology. The nozzle path working as the major part from G-code is generated based on the process parameters such as build orientation, layer height, infill density, etc. Any variations of these parameters may totally change the toolpath in G-code. Other parameters, such as temperature and motion speed, are not related to nozzle path however effecting the total printing time and energy. Therefore, part of the initial models can be built directly from G-code. Other necessary model elements need to be measured from experiments to fill the models, encompassing heating time, environmental temperature, power of major components and real speed of stepper motors.

This study mainly focuses on the consumption predictions based on AM parameters, machine characteristics and G-code, as shown in Fig. 1. In order to improve environmental performance of AM production, the prediction results are utilised as feedback for this cycle to assist users for optimising both design and process parameters.

3.2. Prediction models of time, energy, material consumptions

For FDM 3D printer, an AM task is finished by three core elements: material feeding, heating and extrusion (including hotend and nozzle), and build system (including axis screw, build platform, 4 stepper motors). Fig. 2 illustrates the timeline of an example FDM printing task. At the beginning, heating on build platform (bed) and extruder is to melt the thermoplastic filament continuously and ensure the printed object to attach well on the platform. Once both components reach the target temperature, the material

Table 1
Instructions of a G-code example by Cura slicer software (Smid, 2010).

G-code commands	Instructions
G1 F2400 × 110.432 Y112.065 E5.393	Move nozzle to target position (110.432, 112.065) on X, Y axes at a print speed of 2400 mm/min. The material amount to extrude between the starting point and ending point is 5.393.
G1 × 112.192 Y115.075 E5.476	Move nozzle to target position (112.192, 115.075) on X, Y axes at previous print speed level. The material amount to extrude between the starting point and ending point is 5.476.
G0 F3000 × 77.294 Y94.677	Move nozzle to target position (77.294, 94.677) on X, Y axes at a travel speed of 3000 mm/min;
G0 F6000 Z0.7	Move nozzle on Z axes at a travel speed level of 6000 mm/min;
G1 F1500 E6.14705	Extrude material at a feed rate/speed level of 1500 mm/min. The amount between the starting point and ending point is 6.14705.
G1 F3600	Set the nozzle travel speed to 3600 mm/min.
G92 E0	Set the extruder position/extruded length back to zero.
M140 S70	Set bed temperature to reach target temperature 70 °C
M105	Get bed temperature from temperature sensor
M190 S70	Heat bed to reach target temp
M104 S200	Set extruder temperature to reach target temperature 200 °C
M105	Get extruder temperature from temperature sensor
M109 S200	Heat extruder to reach target temperature 200 °C

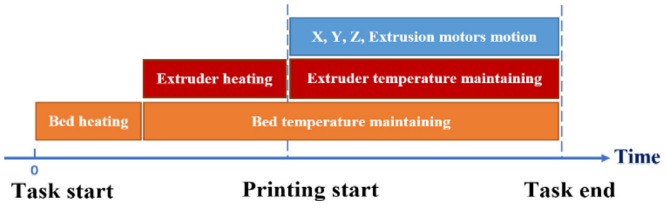

Fig. 2. Example working procedure for basic components by timeline.

deposition begins. The thermoplastic is fed from the spool into the extruder, and the material loading is driven by extrusion motor. Meanwhile the nozzle is responsible for directing the melted material by following the pre-defined trajectory from G-code. Its motion on horizontal platform is driven by X and Y motors. The last motor is used to drive the Z-Axis Screw for vertical motion. During this time, both bed and extruder keep maintaining the temperature till task ends. The working order of those components is decided by printer's properties and G-code instructions.

The energy consumption of 3D printers can be measured by power analyser. This study majorly considers the electricity converted to mechanical and thermal energies. Basic in-range components are summarised in two parts: four stepper motors for material feeding and nozzle motion; bed heating and extruder heating components.

3.2.1. Modelling of stepper motor motions

- Time consumptions of stepper motors

Both print and travel speeds are instructed by F command respectively on different print statuses. Define the print speed is on the status of nozzle moving with material extrusion which refers to the stage of "printing" objects. While the travel speed is on the status of nozzle pure motion without material extrusion.

An initial prediction model is developed according to the G-code commands in Table 1. On the printing status accompanied with material extrusion by G1(X, Y, E) command, t_{xy_e} equals to the time consumed by X, Y and extrusion motor as all three motors run synchronously. Δl_{xy_e} refers to the distance of nozzle motion from the coordinate in last G1 command line to the target coordinate in current command. v_{xy_e} refers to the nozzle speed moving to the target coordinate. The speed value represents the total speed of motor linkage motion. It refers to the speed vector that instructs the X and Y motors with a joint rotation to a specified coordinate in a straight path. Assume that the nozzle travels as constant speed as instructed without considering the accerlation and deceleration. The time is calculated as the extruded length l_e of material divided by print speed v_e, as expressed in (1). Therefore, the total time consumption equals to the accumulation of time for each single print segment.

Similaly, on the status of "travel phase" without material extrusion including G1(X,Y,Z) and G1(X,Y) commands, time consumed by X,Y motors is calculated as the sum of nozzle motion distances Δl_{xy_t} on X,Y axes divided by its travel speed v_t, as shown in (2). Time consumed by Z motor is calculated as the object height l_z, which also refers to the vertical moving distances on Z axis, divided by Z motor speed v_z, as shown in (3). For different 3D printers, v_z generally equals to travel speed v_t, or is set as a fixed constant.

$$t_{xy_e} = \sum \frac{\Delta l_{xy_e}}{v_{xy_e}} = \frac{l_e}{v_e} \tag{1}$$

$$t_{xy_t} = \sum \frac{\Delta l_{xy_t}}{v_t} \tag{2}$$

$$t_z = \frac{l_z}{v_z} \tag{3}$$

• Powers of stepper motors

Energy consumption is calculated by the product of power and time. Assume that the motor power is related to the motor speed (print or travel speed) during printing process. The power of each motor running at different levels of speed requires external experimental measurements by using the power analyser. Thus, the initial expressions of motor power are temporarily presented as below.

$$P_{xy} = f_{xy}(v_{xy}) \tag{4}$$

$$P_e = f_e(v_e) \tag{5}$$

$$P_z = f_z(v_z) \tag{6}$$

3.2.2. Modelling of bed and extruder heating

• Time consumptions of bed and extruder heating

Time calculation of heating process is separated as two parts: one is for heating the extruder and build platform (bed) to the target temperature. This process is named as "initial heating phase". The consumed time t_{EH_l} for extruder heating and t_{BH_l} for bed heating are the functions of temperature differences ΔT_{EH} and ΔT_{BH} rising from current temperature T_0 to target temperatures T_{EH} and T_{BH}, as shown in (7)–(10). The correlations are measured through experiment. The other phase is to maintain components heating at target temperature, also named as "temperature maintaining phase". Assume that heating is continuously maintained through the entire printing process. Thus, consumed time t_{EH} and t_{BH} equal to the consumptions of entire print task which can be obtained from previous section, as shown in (11).

$$\Delta T_{EH} = T_{EH} - T_0 \tag{7}$$

$$\Delta T_{BH} = T_{BH} - T_0 \tag{8}$$

$$t_{EH_l} = g_{EH_l}(\Delta T_{EH}) \tag{9}$$

$$t_{BH_l} = g_{BH_l}(\Delta T_{BH}) \tag{10}$$

$$t_{EH} = t_{BH} = t_{xy_e} + t_{xy_t} + t_z \tag{11}$$

• Powers of bed and extruder heating

Heating powers of two components are related to the target temperature, as shown from (12)–(15). The relations can be determined through experiments by using power analyser.

$$P_{EH_l} = f_{EH_l}(T_{EH}) \tag{12}$$

$$P_{EH} = f_{EH}(T_{EH}) \tag{13}$$

$$P_{BH_l} = f_{BH_l}(T_{BH}) \tag{14}$$

$$P_{BH} = f_{BH}(T_{BH}) \tag{15}$$

• Powers of setup and standby modes

3D printer has a stable power supply on the status of standby mode. Once a printing task starts, power supply is increased up to a higher value for running the machine. This phase is defined as "setup" mode. In this study, power of standby mode P_s and setup mode P_0 are both measured as constants throughout the entire task according to subsequent experimental results.

3.2.3. Summary of total consumptions

The total consumptions are expressed below. r refers to the diameter of material filament, the extruded length l_e of material can be obtained from G-code file.

• Total time consumption:

$$t_{total} = t_{xy_e} + t_{xy_t} + t_z + t_{EH_l} + t_{BH_l} \tag{16}$$

• Total material consumption:

$$V_{total} = l_e \pi \left(\frac{r}{2}\right)^2 \tag{17}$$

• Total energy consumption:

$$E_{total} = P_{xy}(t_{xy_e} + t_{xy_t}) + P_z t_z + P_e t_e + P_{EH_l} t_{EH_l} + P_{EH} t_{EH} + P_{BH_l} t_{BH_l} + P_{BH} t_{BH} + (P_s + P_0)\, t_{total} \tag{18}$$

The nozzle motion distances can be calculated from G-code. Due to machine specificity, necessary model elements and correlations between powers and machine parameters require experiments for the model refinement, including:

- Powers of four stepper motors at different speeds.
- Powers of bed and extruder heating, and temperature maintaining at different target temperatures.
- Powers of standby and setup modes.
- Time to heat bed and extruder at different temperature differences.
- Current temperature at the beginning of each task.
- Real speeds of X, Y, Z motors based on corresponding ideal speeds.

The experiments can ensure the accuracy of prediction results. To minimise the workload, only a small number of tests are performed in this study. The obtained data is processed with the assist of curve fitting tool. It may facilitate the predictions to be accomplished directly through G-code files without additional experiments. To verify model accuracy, a case study is provided in Section 3.

4. Case study

4.1. Experimental setup

ANYCUBIC i3 Mega is a commonly used FDM printer from ANYCUBIC. Its supporting slicer software Cura is developed byUltimaker by using G-code as an open-source code. The equipment to measure the apparent powers of basic components is CW500, a portable power metre from Yokogawa Test & Measurement Company. Its supporting software CW500 Viewer enables the analysis of recorded data in the format of scatter plot. Specifications are listed in Table 2 and Table 3.

4.2. Prediction models

Fig. 3 illustrates the power plot of an example FDM task. The total energy is calculated as the sum of energy-consumed components cooperating together. During experiments, the total power (first plot in Fig. 3) was separated to be measured based on each single component and different working modes.

• Powers of setup and standby modes

All measured results are presented in Table 4. It was found that the standby power P_s and setup power P_0 were measured as fixed constants throughout the entire task which were not affected by process parameters or components.

• Time, power of bed and extruder heating

Table 2
Specifications of ANYCUBIC i3 Mega 3D printer.

Supported material	PLA, ABS, HIPS, Wood	Extruder quantity	Single
Build size	210 × 210 × 205 (mm^3)	Printer dimensions	405 × 410 × 453 (mm^3)
Layer resolution	0.04–0.3 mm	Infill density	2–100%
Bed temperature	0–130 °C	Nozzle diameter	0.4 mm
Filament diameter	1.75 mm	Extruder temperature	0–285 °C
Print speed	0.2–150 mm/s	PLA temperature	180–220 °C
Z axis speed	5 mm/s	Travel speed	0.1–300 mm/s

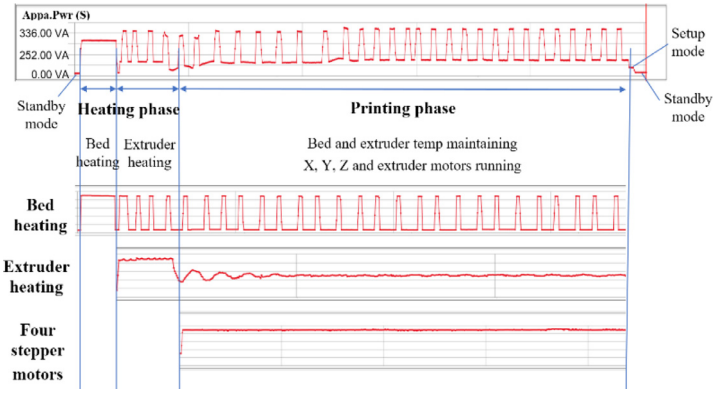

Fig. 3. Power plot of an AM task printed by ANYCUBIC i3 Mega 3D printer.

Table 3
Specifications of CW500 power quality analyser.

Sampling rate	24μs
Voltage range	600V
Current Clamp range	50A
Record interval range	1s-10$mins$

In the phase of initial heating, it was discovered that the power values of bed P_{BH_I} and extruder heating P_{EH_I} were stabilised as fixed constants. The corresponding time $t_{EH_I}$and t_{BH_I} were individually related to the target temperatures of bed and extruder (T_{BH} and T_{EH}).

In the phase of temperature maintaining for extruder, the measured power P_{EH} of extruder temperature maintaining was stabilised and was related to the target temperature T_{EH}.

In the phase of temperature maintaining for bed, it was found that extruder heating was behind bed heating. Thus, the time of bed temperature maintaining t_{BH} concluded the total printing time and the extruder heating time t_{EH_I}, as expressed in (19). The power of bed temperature maintaining was distributed in the pulse format with a fixed cycle. Due to the characteristics of i3 Mega machine, the power was supplied by pulse currents for intermittent heating to maintain the bed temperature. In order to simplify the modelling, the energy E_{BH} was calculated by the average energy per cycle E_{bh} multiplied its average cycle time t_{cycle}, as shown in (20). E_{bh} was measured as an average constant while t_{cycle} was related to the target temperature T_{BH}.

In printing phase, the power P_{motor} of four stepper motors' linkage motion was measured as a fixed constant. The relations between real speeds v_x, v_y, v_z and their ideal speeds $v_{x_{ideal}}$, $v_{y_{ideal}}$, $v_{z_{ideal}}$ of X, Y, Z motors were determined from experimental data, as shown in Table 4.

$$t_{BH} = t_{xy_e} + t_{xy_t} + t_z + t_{EH_I} \tag{19}$$

$$E_{BH} = E_{bh}\frac{t_{xy_e} + t_{xy_t} + t_z + t_{EH_I}}{t_{cycle}} \tag{20}$$

All experiment results and required functional correlations determined by curve fitting tool were summarised in Table 4. In con-

Table 4
Experimental results of practical power, time and speed of Anycubic i3 Mega 3D printer components.

Standby mode power P_s	18.47357VA
Setup mode power P_0	9.58706VA
Extruder initial heating power P_{EH_I}	82.23392VA
Bed initial heating power P_{BH_I}	262.07253VA
Stepper motor power P_{motor}	42.47047VA
Bed maintaining heating energy per cycle E_{bh}	1331.00922J
Real speed of Z motor v_z	5.94827(mm/s)

Fitting correlations according to experimental results		R-square
Bed initial heating time t_{BH_I}	$t_{BH_I} = 4.778(T_{BH} - T_{B0}) - 10.4$	0.96240
Extruder initial heating time t_{EH_I}	$t_{EH_I} = 0.2834(T_{EH} - T_{E0}) + 10.29$	0.99200
Bed maintaining temperature time per cycle t_{cycle}	$t_{cycle} = 0.03306{T_{BH}}^2 - 4.839T_{BH} + 193$	1.00000
Extruder maintaining temperature power P_{EH}	$P_{EH} = 0.00376{T_{EH}}^2 - 1.275T_{EH} + 140.1$	1.00000
Real speed of X motor v_x	$v_x = -0.001106{v_{x_{ideal}}}^2 + 1.058v_{x_{ideal}} - 0.6637$	1.00000
Real speed of Y motor v_y	$v_y = -0.0017{v_{y_{ideal}}}^2 + 1.108v_{y_{ideal}} - 1.647$	1.00000

Table 5
Prediction model inputs of Anycubic i3 Mega 3D printer.

Model inputs	Comments	Test 1	Test 2
T_{B0}	Current bed temperature (°C)	22	23
T_{E0}	Current extruder temperature (°C)	22	22
T_{BH}	Bed target temperatures (°C)	60	53
T_{EH}	Extruder target temperature (°C)	200	180
v_e	Print and extrusion speed (mm/s)	60	72
v_t	Nozzle travel speed (mm/s)	120	130
v_z	Build platform speed (mm/s)	120	130
h	Layer thickness (mm)	0.04	0.04
I_d	Infill density	25%	25%

Table 6
Prediction results and experimental results in test 1.

Model outputs	Value	Experimental results	Deviation ratio
Time (s)	3049.40426	3149.00000	3.16277%
Energy (J)	531,469.98655	579,979.80000	8.36405%
Material (mm^3)	2110.41528	1960.19715	−7.66342%
		Software 2109.34607	−0.05069%

Table 7
Prediction results and experimental results in test 2.

Model outputs	Value	Experimental results	Deviation ratio
Time (s)	2121.32770	2245.00000	5.50879%
Energy (J)	333,463.42432	364,326.57000	8.47129%
Material (mm^3)	1778.50421	1612.99560	−10.26095%
		Software 1770.39009	−0.04583%

clusion, the total time, energy and material consumptions are expressed below.

- Total time consumption:

$$t_{total} = t_{xy_e} + t_{xy_t} + t_z + t_{EH_l} + t_{BH_l} \tag{21}$$

- Total energy consumption:

$$E_{total} = P_{motor}(t_{xy_e} + t_{xy_t} + t_z) + P_{EH_l}t_{EH_l} + P_{EH}t_{EH} + P_{BH_l}t_{BH_l} + E_{BH} + (P_s + P_0)\ t_{total} \tag{22}$$

- Total material consumption:

$$V_{total} = l_e\pi\left(\frac{r}{2}\right)^2 \tag{23}$$

$$r = 1.75mm \tag{24}$$

4.3. Prediction and experiment results

Tests of two design models with different printer parameters were performed to validate the model precision. Customised parameters in Table 5 were defined as inputs of the prediction models. Meanwhile, consumptions in practical printing task was measured to determine the deviation ratios between prediction results and actual results. All results were presented in Table 6 and 7.

Compared with time consumption, due to the uncertainty of heating component, the energy deviation was found to be greater. The thermometer used to monitor the temperature was lack of accuracy, resulting in unstable heating throughout the printing process. The prediction of material consumption was compared with two experimental results. One was measured from practical tests. The high deviation was caused by the out-of-step problem of extrusion motor. As the motor load was relatively high by loading material filament, its real speed was affected and was lower than the ideal speed. Unlike X, Y, and Z motors, the speed value was difficult to test because it was only responsible for loading the material instead of controlling the nozzle movement. Therefore, in this study, material predictions were established under ideal conditions.

The other one was determined by the slicer software. The model output was closer to this result because they were both calculated under the ideal conditions. However, this result only considered the material consumption for the build design. It ignored the material usage of preparation stage. The prediction model considered the materials used in the entire task, and therefore achieves higher accuracy.

5. Future work

Processing parameters will be optimised based on prediction results to achieve the lowest consumptions. Acceleration and deceleration of nozzle motion will be considered to further improve the model accuracy. The real speed measurement of extrusion motor will continue to reduce the deviation rate of material prediction. In addition, machine learning methods will be considered to improve prediction models in real time.

CRediT authorship contribution statement

Jimeng Yang: Conceptualization, Methodology, Software, Resources, Validation, Formal analysis, Visualization, Writing - original draft, Data curation, Investigation. **Ying Liu:** Conceptualization, Funding acquisition, Methodology, Project administration, Supervision, Validation, Writing - review & editing.

Acknowledgements

I would like to thank the University of Glasgow for providing the lab and equipment.

References

Apro, Karlo, 2008. Secrets of 5-axis Machining. Industrial Press Inc.
Balogun, V.A., Kirkwood, N., Mativenga, P.T., 2015. Energy consumption and carbon footprint analysis of fused deposition modelling: a case study of RP Stratasys Dimension SST FDM. Int. J. Sci. Eng. Res. 6 (8), 442–447.
Chua C, K., Leong K, F, 2014. 3D printing and additive manufacturing: principles and applications (with companion media pack) of rapid prototyping fourth edition. World Scientific Publishing Company.
Fok K, Y., Cheng C, T., Chi K, T., et al., 2016. A relaxation scheme for TSP-based 3D printing path optimizer. In: 2016 International Conference on Cyber-Enabled Distributed Computing and Knowledge Discovery (CyberC). IEEE, pp. 382–385.
Ford, S., Despeisse, M., 2016. Additive manufacturing and sustainability: an exploratory study of the advantages and challenges. J. Clean. Prod. 137, 1573–1587.
Huang, Runze, et al., 2016. Energy and emissions saving potential of additive manufacturing: the case of lightweight aircraft components. J. Clean. Prod. 135, 1559–1570.
Kellens, K., Baumers, M., Gutowski, T.G., Flanagan, W., Lifset, R., Duflou, J.R., 2017. Environmental dimensions of additive manufacturing: mapping application domains and their environmental implications. J. Ind. Ecol. 21, S49–S68. doi:10.1111/jiec.12629.
Li, Q., Kucukkoc, I., Zhang, D.Z., 2017. Production planning in additive manufacturing and 3D printing. Comput. Oper. Res. 83, 157–172.
Meteyer, S., Xu, X., Perry, N., et al., 2014. Energy and material flow analysis of binder-jetting additive manufacturing processes. Proc. CIRP 15, 19–25.
Peng, T., Sun, W., 2017. Energy modelling for FDM 3D printing from a life cycle perspective. Int. J. Manuf. Res. 12 (1), 83–98.
Smid, Peter, 2010. CNC Control Setup For Milling and turning: Mastering CNC Control Systems. Industrial Press Inc.
Watson J, K., Taminger K M, B, 2015. A decision-support model for selecting additive manufacturing versus subtractive manufacturing based on energy consumption. J. Clean. Prod..
Yang, J., Chen, Y., Huang, W., et al., 2017. Survey on artificial intelligence for additive manufacturing. In: 2017 23rd International Conference on Automation and Computing (ICAC). IEEE, pp. 1–6.
Yoon H, S., Lee J, Y., Kim H, S., et al., 2014. A comparison of energy consumption in bulk forming, subtractive, and additive processes: review and case study. Int. J. Precis. Eng. Manuf.-Green Technol. 1 (3), 261–279.